UC Berkeley
UC Berkeley Previously Published Works

Title

Pharmacologically Stimulated Pupil and Accommodative Changes in Guinea PigsPharmacologically Stimulated Accommodation in Guinea Pigs

Permalink

https://escholarship.org/uc/item/026107tg

Journal

ISSN

Authors

Ostrin, Lisa A
Garcia, Mariana B
Choh, Vivian
et al.

Publication Date

2014-08-28

DOI

Peer reviewed

Pharmacologically Stimulated Pupil and Accommodative Changes in Guinea Pigs

Lisa A. Ostrin,[1] Mariana B. Garcia,[2] Vivian Choh,[3] and Christine F. Wildsoet[2]

[1]University of Houston College of Optometry, Houston, Texas, United States
[2]University of California Berkeley School of Optometry, Berkeley, California, United States
[3]University of Waterloo Optometry and Vision Science, Waterloo, Ontario, Canada

PURPOSE. The guinea pig is being used increasingly as a model of human myopia. As accommodation may influence the effects of manipulations used in experimental myopia models, understanding the accommodative ability of guinea pigs is important. Here, nonselective muscarinic agonists were used as pharmacological tools to study guinea pig accommodation.

METHODS. Measurements were made on 15 pigmented guinea pigs. For in vivo testing, animals were anesthetized and, following baseline measurements, 2% pilocarpine was applied topically. Measurements included A-scan ultrasonography, optical coherence tomography (OCT) imaging, corneal topography, and refraction. In vitro lens scanning experiments were performed using anterior segment preparations, with measurements before and during exposure to carbachol. Anterior segment structures were examined histologically and immunohistochemistry was done to characterize the muscarinic receptor subtypes present.

RESULTS. In vivo, pilocarpine induced a myopic shift in refractive error coupled to a small, but consistent decrease in anterior chamber depth (ACD), a smaller and more variable increase in lens thickness, and a decrease in pupil size. Lens thickness increases were short-lived (10 minutes), while ACD and pupil size decreased over 20 minutes. Corneal curvature was not significantly affected. Carbachol tested on anterior segment preparations in vitro was without effect on lens back vertex distance, but did stimulate pupil constriction. Immunohistochemistry indicated the presence of muscarinic receptor subtypes 1 to 5 in the iris and ciliary body.

CONCLUSIONS. The observed pilocarpine-induced changes in ACD, lens thickness, and refraction are consistent with active accommodation in the guinea pig, through cholinergic muscarinic stimulation.

Keywords: accommodation, guinea pig, anterior segment, muscarinic agonists, pupil size

The guinea pig is being used increasingly as a model of human myopia,[1-3] yet its accommodative ability has not been well characterized. Accommodation remains of relevance to this field, given the widespread use of negative lenses to impose retinal defocus, by way of inducing myopia in animal models. As accommodation may modify the defocus experience of the retina, understanding the retinal image characteristics driving lens-induced myopia necessarily requires an understanding of the accommodative ability of an animal. To date, to our knowledge there has been no systematic evaluation of accommodation in the guinea pig.

The guinea pig is a diurnal, precocial mammal (i.e., well developed at birth). It is able to emmetropize, that is, adjust its ocular growth to eliminate neonatal refractive errors, in a manner similar to many other animals, including humans,[4] and it is susceptible to form deprivation and lens-induced experimental myopia.[1,2] Interestingly, in a strain of wild-type guinea pigs with spontaneous myopia, attempts to elicit an accommodative response to a near fixation target were unsuccessful.[5] However, in another study, refractions measured with retinoscopy were reported to be more hyperopic when accommodation was inhibited with cyclopentolate, by an average of +3.00 diopters (D), implying the presence of tonic accommodation.[4]

Of other commonly used animal models for human myopia (chick,[6] monkey,[7] and tree shrew[8]) young chicks have the most impressive accommodative ability, with amplitudes as high as 25 D reported.[9-11] This high amplitude reflects, in part, the recruitment of the cornea as well as the crystalline lens during accommodation; specifically, when the ciliary muscle contracts, corneal steepening accompanies the increased curvature of both surfaces of the crystalline lens. The pharmacology of avian accommodation also is different because the ciliary muscle is comprised of striated instead of smooth muscle, with nicotinic receptors instead of muscarinic receptors (mAChRs), as found on smooth muscle.[10,12]

Not all mammals exhibit accommodation. Among the exceptions is the gray squirrel, which shows no change in refraction in response to muscarinic agonists.[13] This contrasts with the increases in accommodation found in response to muscarinic agonists in most mammals, including humans.[7,14] Nonetheless, squirrels are susceptible to experimental form deprivation myopia.[13] Mice, which have been used in some more recent experimental myopia[15] and related genetic[16-20] studies, also appear to be without accommodation.[21] That guinea pigs belong to the rodent family further argues for a study of the type reported here, which is aimed at providing a

TABLE 1. Summary of Experiments, Including Drug Treatments, Measurements Made and Sample Specifications

Experiment	Measurement and Instrument	Ages, mo (*n* of Eyes)
In vivo stimulation of accommodation		
Pilocarpine, 2%, 3 topical instillations	High frequency A-scan ultrasonography, custom-built instrument	2 (2)
		6 (2)
		16 (2)
Pilocarpine, 2%, 3 topical instillations	Anterior segment OCT imaging, Visante	2 (2)
		6 (2)
		12 (2)
		16 (2)
Pilocarpine, 2%, 3 topical instillations	Corneal topography, Topcon	2 (2)
		6 (2)
		16 (2)
Pilocarpine, 2%, 3 topical instillations	Refraction, Hartinger refractometer	3 (3)
		6 (2)
In vitro stimulation of accommodation		
Carbachol	Lens scanning, Scantox	~6 (4)
Histology		
Immunohistochemistry	Immunohistochemistry for M1, 2, 3, 4 and 5	~3 (1)
Anterior segment imaging	Gross morphology	~3 (1)
H&E stained sections	Ciliary body morphology	2 (1)

better understanding of the functional capability of one rodent used as a myopia model.

The guinea pig iris and ciliary body have been shown to contain muscarinic receptors, similar to those of other mammals and primates.[22–24] In the current study, pilocarpine and carbachol, which are nonselective muscarinic receptor agonists, were used to look for evidence of accommodation in the guinea pig, in vivo and in vitro. Drug-induced changes in anterior ocular segment structures, including pupil size, were evaluated and changes in refractions were measured as a proxy for accommodative changes. Immunohistochemistry was used to confirm the presence and evaluate the subtypes of muscarinic receptors on the ciliary body and iris.

METHODS

This study used 15 pigmented guinea pigs (*Cavia porcellus*), ranging in age from 2 to 16 months. Three of the animals were used for histological and immunohistochemical studies of the anterior segment. Details of the experiments, including the age of animals at testing, are summarized in Table 1. Protocols were approved by the University of California, Berkeley Animal Care and Use Committee and conformed to the ARVO statement for the Use of Animals in Ophthalmic and Vision Research.

In Vivo Pilocarpine-Induced Accommodation

To study accommodation in vivo, measurements were made on one eye of each animal, which underwent up to four recording sessions, separated by at least one week. Measurements included refraction, high frequency A-scan ultrasonography, anterior segment optical coherence tomography (OCT) imaging, and corneal topography; the protocols for which are described below. Only one type of measurement was done in each session. In all cases, animals were first anesthetized with ketamine (30 mg/mL) and xylazine (3 mg/mL), and the test eye held open with a lid speculum. Topical 2% pilocarpine (Alcon, Ft. Worth, TX, USA), a nonselective muscarinic agonist, was used to stimulate accommodation. For all measurements, the same dosing regimen was used, comprising 2 drops applied every 4 minutes for a total of 6 drops, and preceded by baseline measurements. Additional measurements were taken over a 20-

minute period following the instillation of the drops. Guinea pigs were wrapped in a blanket over this period and placed on a heating pad immediately afterward to maintain body temperature until fully recovered from anesthesia. The corneas were irrigated frequently with a saline solution to maintain clarity.

Refraction. A Hartinger Coincidence Refractometer (Carl Zeiss Meditec, Jena, Germany) was used to measure the refractive errors of anesthetized animals, which were positioned on a custom-designed stage in front of the instrument. The optical axis of the eye was aligned with that of the instrument. Measurements were made before (baseline), during, and after completion of the pilocarpine treatment regimen, at 2-minute intervals out to 20 minutes. Differences between baseline refractive errors and subsequent readings were taken to represent accommodative responses.

High-Frequency A-Scan Ultrasonography. Axial ocular dimensions, including anterior chamber depth (ACD) and lens thickness (LT), were measured using this technique, which has been described in detail previously.[3,25] In brief, the anesthetized animal was positioned prone on a custom-designed stage. The ultrasound probe was brought into contact with ultrasound gel on the cornea and aligned with the optical axis of the eye with the aid of an x-y-z micromanipulator attached to the probe. The position of the eye was monitored continuously to ensure it remained appropriately aligned over the course of measurements. Rather than removing the probe to allow the instillation of pilocarpine, drops were applied to the peripheral cornea by use of a cannula. Measurements were made at intervals of 2 minutes, with approximately 15 traces captured each time. Reported results represent the average of at least 10 traces for each time point.

Anterior Segment OCT Imaging. Pupil size and ACD data were collected using a noncontact OCT imaging system (Visante, Carl Zeiss Meditec, Inc., Dublin, CA, USA). For imaging, anesthetized animals were placed on a custom-designed stage to facilitate ocular alignment. After baseline imaging, pilocarpine dosing was started and the treated eye imaged at 1-minute intervals over the next 20 minutes. Calipers built into the Visante instrument software were used to measure pupil size and ACD, as indices of pilocarpine-induced changes. Attempts were made also to quantify ciliary body shape changes, as published previously in humans.[26,27]

However, since the boundary of the ciliary body could not be identified consistently in the OCT images, this type of analysis was not considered further.

Corneal Topography. Corneal curvature data were captured using a corneal topographer (WavefrontSG; Topcon Medical Systems, Inc., Oakland, NJ, USA) in anesthetized animals, which were hand-held in front of the instrument and aligned with the instrument's optics. In addition to baseline measurements, data were collected every 2 minutes. At each time-point, three to five measurements were recorded and averaged to determine corneal power. Corneal power was derived from the algorithm built into the instrument, corresponding to an approximate 4.5 mm diameter central corneal zone. While this instrument was designed for human eyes, the index of refraction of the guinea pig cornea is thought to be similar to humans, and, thus, no correction to the raw data was undertaken.[4]

In Vitro Carbachol-Induced Accommodation

This in vitro experiment made use of a ScanTox (ver. 2.0.154; XTOX Scientific, Neoean, Ontario, Canada), a scanning laser system specifically designed for this purpose.[6] In brief, the instrument comprises a chamber for mounting an anterior ocular segment through which a low-power helium-neon laser beam is directed. A computer-controlled stepper motor is linked to the laser, allowing the position of the laser beam to be moved, stepwise, in a radial direction away from the optic axis to the limit imposed by the pupil boundary. A video camera captured images of the laser's path through the mounted preparation, from which points of intersection of the rays with the optical axis were identified and averaged to determine the back vertex distance (BVD) using this system's software. The step size was set to capture approximately 20 to 25 beam paths within the pupil (0.1–0.16 mm step size). Pupil size was derived from the number of beams passing through the lens and step size setting.

Enucleated eyes from 4 guinea pigs sacrificed with a lethal dose of sodium pentobarbital (Euthasol; Virbac Animal Health, Ft. Worth, TX, USA) were used in this part of the study. One eye from each animal was bisected at the equator, posterior to the ciliary processes to isolate the anterior segment, which then was placed on a Sylgard washer with the cornea facing down and sclera pinned in place. The mounted anterior segment was transferred to the silicone base plate of the ScanTox chamber, which then was filled with 20 mL oxygenated Tyrode's solution with 5% fetal bovine serum (FBS) added to allow visualization of the laser beam passing through the chamber. Baseline scans were captured from all four preparations and two of these preparations were rescanned 20 minutes after replacement of the Tyrode's solution with an equivalent solution containing 10 mM carbachol. Carbachol was chosen over pilocarpine for this study because of its longer duration of action. Both drugs are nonselective muscarinic agonists, although carbachol also shows additional nicotinic agonist activity.[28] Because the refracting power of the cornea is neutralized by the bathing solution, observed refraction changes reflect lens changes only.

Anterior Segment Histology and Immunohistochemistry

Three guinea pigs were sacrificed for histology. Following euthanasia via intracardiac injection of sodium pentobarbital, the eyes of one guinea pig were enucleated and fixed overnight at 4°C in a solution of 4% paraformaldehyde and 3% sucrose, then cryoprotected in 20% sucrose at 4°C for 6 hours, before being embedded in a 1:1 solution of OCT and 20% sucrose.
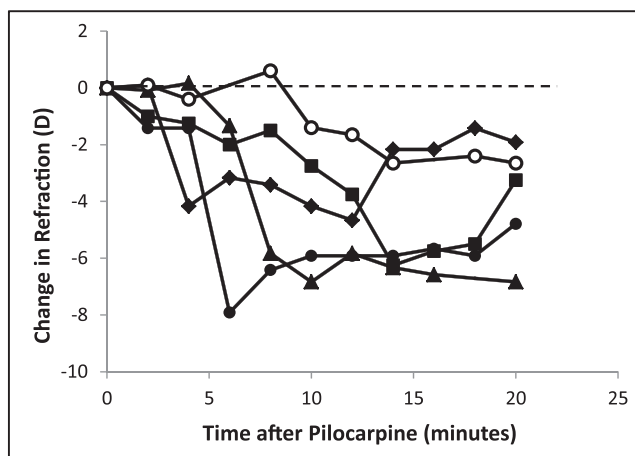
FIGURE 1. Changes in the refractions of individual animals following topical application of pilocarpine, normalized to baseline (no drug) values ($n = 5$). *Lines* represent data from individual animals.

They then were snap frozen with liquid nitrogen. Cryostat sections (8 μm) of the anterior segment were cut at −20°. Commercial immunofluorescent assay kits for AChMs, subtypes 1, 2, 3, 4, and 5 (IFA muscarinic receptor kits; Research & Diagnostic Antibodies, Benicia, CA, USA) were used to label muscarinic receptors. Nuclei were counterstained with 4′, 6-diamindino-2-phenylinole (DAPI). Images of ciliary muscle, iris and peripheral retina were captured as z-stacks through appropriate filters for DAPI and FITC fluorescence; z-stacks were later deconvolved and shown as a projection using a DeltaVision Spectris deconvolution microscope (Applied Precision, Issequah, WA, USA). Two controls were used to evaluate the specificity of the immunostaining. First, to evaluate autofluorescence, an unstained section was viewed with the wavelength used to excite FITC, and the same exposure and intensity as used to view stained sections. Secondly, for each receptor subtype, control sections were prepared by first incubating the primary antibody with a synthetic muscarinic receptor of matching subtype, and then incubating the sections in the primary antibody/synthetic receptor solution. For each subtype and each tissue, control sections were compared to experimental sections using matched exposure and intensity. Equivalent sections were compared and the intensity of fluorescence given a subjective rating on a scale of 1 to 3.

To characterize the ciliary muscle architecture, the enucleated fixed eyes of another guinea pig were paraffin-embedded, and prepared sections processed for hematoxylin and eosin (H&E) staining and then imaged. In addition, a third eye was bisected at the equator and the posterior view of the anterior segments photographed through a surgical microscope (Stereomicroscope SZX16A; Olympus, Center Valley, PA, USA) to better visualize the gross morphology of the ciliary processes and attached zonular fibers.

RESULTS

In Vivo Pilocarpine-Induced Accommodation

In all animals ($n = 5$, aged 3–6 months), pilocarpine induced a relative myopic shift in refractive error, confirming that guinea pigs do have accommodation. Baseline refractions for these guinea pigs, measured with the Hartinger Refractometer, were +1.7 ± 0.76 D. Accommodative amplitude, estimated as the maximum difference in refractive errors measured before and
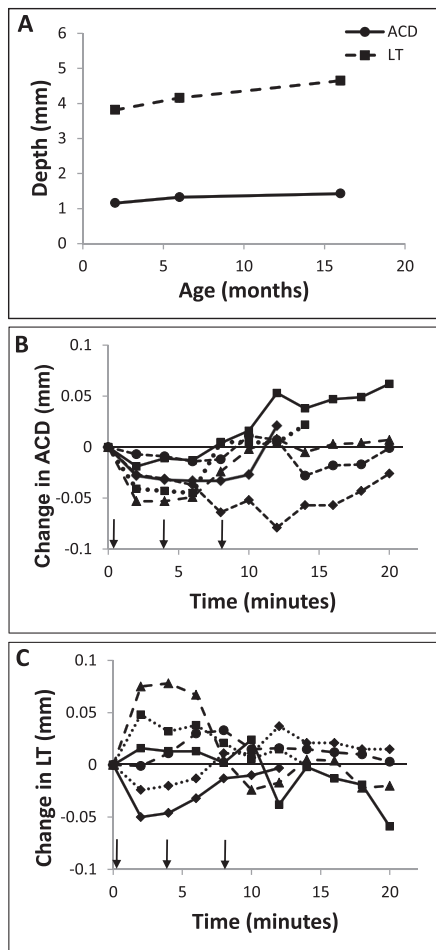
FIGURE 2. (A) Mean baseline ACD (*solid line*) and LT (*dashed line*), measured with high frequency A-scan ultrasonography, with animal age ($n = 2$ for each age, *error bars* are within the symbols); changes from baseline in (B) ACD and (C) LT following application of topical 2% pilocarpine drops ($n = 6$); *arrows* indicate timing of drops.
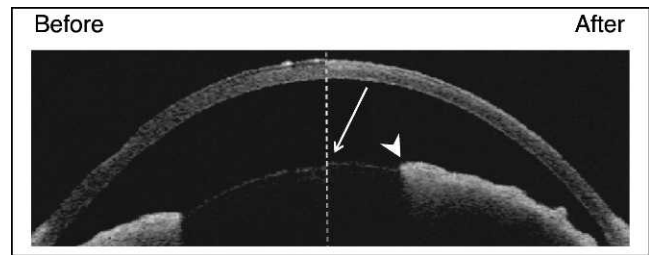

FIGURE 3. Anterior segment images captured before and 15 minutes after application of pilocarpine; *arrow* indicates the advance in anterior surface lens toward the cornea, decreasing the ACD; the centripetal advance of pupil margin also is evident (*arrowhead*).

after the instillation of pilocarpine (Fig. 1), averaged 5.65 ± 2.0 D, with individual animals reaching their maximum values between 4 and 14 minutes after instillation of the first drops.

Consistent with the above refraction results, biometry data collected using A-scan ultrasonography revealed drug-induced changes in anterior segment dimensions. In response to topical pilocarpine, there was a transient increase in LT coupled to a decrease in ACD. The ACD decreased from a baseline average of 1.30 ± 0.12 mm to a minimum of 1.28 ± 0.12 mm (−1.54%) 8 minutes after the instillation of the first drops of pilocarpine. These changes in ACD had reversed by the end of the monitoring period (1.32 ± 0.12 mm, $t = 20$ minutes, Fig. 2B). The decrease in ACD was quite small (mean, 0.02 mm at $t = 8$ minutes), but was highly significant ($P < 0.005$, paired t-test). The changes in LT also were small and in the opposite direction to those in the ACD, with a similar time frame. The LT increased from a baseline average of 4.19 ± 0.40 to 4.20 ± 0.41 mm after 8 minutes (+0.24%), before returning to baseline dimensions (4.19 ± 55 mm at $t = 20$ minutes, Fig. 2C). Compared to changes in ACD, the mean increase in LT was smaller (0.01 mm, reached after 8 minutes) and did not achieve statistical significance ($P = 0.19$). The distance between the cornea and posterior surface of the lens did not significantly change over the 20-minute monitoring period (mean change, 0.003 ± 0.014 mm, $P = 0.59$), implying that the ACD changes

were at least partly a byproduct of LT changes. Note that no age-related differences in accommodation were detected, perhaps reflecting our small sample size, although age-related differences in baseline ocular dimensions were documented. Specifically, ACD and LT increased slightly with age from 2 to 16 months ($n = 6$, Fig. 2A).

Anterior segment OCT imaging confirmed the above finding of a decrease in ACD with pilocarpine and allowed quantification of pilocarpine-induced pupil meiosis, which also was apparent on casual inspection ($n = 8$). The ACD decreased from a baseline value of 1.12 ± 0.11 to 1.07 ± 0.12 mm after 20 minutes. This 0.05-mm change represents a decrease to 95.5% of the baseline value (Figs. 3, 4A). The change measured with OCT imaging was larger and more sustained than observed with ultrasonography. Reduced pilocarpine transfer across the cornea due to the continuous presence of ultrasound gel on the cornea during the latter measurements offers a potential explanation for this difference. Pupil size decreased to approximately 63% of the baseline value over the same time period, from 4.03 ± 0.50 to 2.54 ± 0.14 mm (Fig. 4B). The changes in ACD and pupil size showed an approximately linear relation ($r^2 = 0.44$, $P = 0.11$, Fig. 4C), consistent with their similar temporal profiles. Only one animal, which also was the oldest (16 months), demonstrated a decrease in pupil size without any change in ACD.

Corneal curvature, as assessed by corneal topography, was not altered significantly by pilocarpine ($n = 6$); corneal powers measured at baseline and 20 minutes after instillation of the first drops averaged 83.7 ± 7.9 and 84.8 ± 7.6 D, respectively (mean change, 1.1 D; $P = 0.12$, paired t-test). Thus, the cornea does not appear to contribute to accommodation in the guinea pig.

In Vitro Carbachol-Induced Accommodation

This in vitro lens scanning experiment was aimed at providing direct information about the contribution to lenticular shape changes in the guinea pig. In addition, it provides information about the optical quality of its crystalline lens. The lens scanning preparation is shown in Figure 5A. All lenses exhibited negative spherical aberration (SA) as reflected in respective positions of the planes of focus of paraxial and peripheral rays (Fig. 5B), the latter being 1.5 ± 0.7 mm beyond the former on average. The mean baseline lens BVD for the four eyes tested was 8.25 ± 0.24 mm, based on all rays falling within the natural pupil, which had an average diameter of 3.88 ± 0.7 mm.

For the two preparations scanned before and during incubation in 10 mM carbachol, pupil size decreased from 4.4 and 3.4 mm to 1.7 and 1.2 mm, respectively. The BVDs decreased from baseline values of 8.51 and 8.34 mm to 7.95 and 7.95 mm, respectively, when all rays falling within the
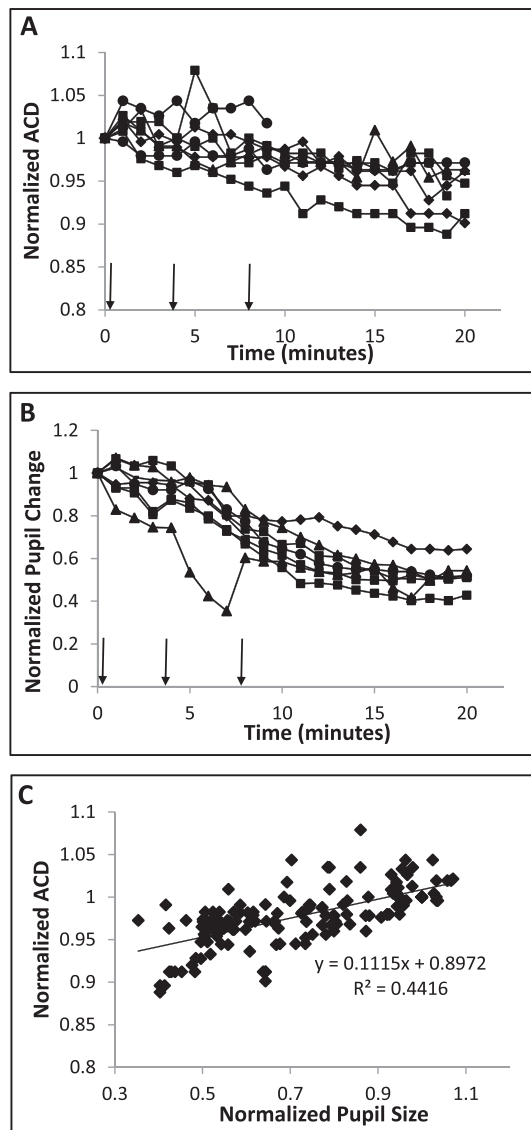
FIGURE 4. Changes in (**A**) ACD and (**B**) pupil size following topical application of 2% pilocarpine drops, as measured from anterior segment OCT images and referenced to baseline values for each subject, and each *line* represents records from one animal; *arrows* indicate timing of drops. (**C**) Induced pupil size and ACD decreases followed similar temporal patterns, as evidenced by the linear relationship between the changes in each parameter (*n* = 8).

pupil in each of the two conditions were considered. However, when calculations were limited to comparable pupillary zones, that is, paraxial rays passing through the central 1.2 mm zone of the pupil, no significant effect of carbachol on BVD was observed (Figs. 5C, 5D).

Anterior Segment Histology and Immunohistochemistry

Morphologically, the ciliary body was found to have well-developed ciliary processes of variable lengths with distinct ciliary ridges extended toward, but not making contact with, the equatorial edge of the lens (Fig. 6A). The ciliary processes also are clearly visible in histological sections, in which the ciliary muscle within the ciliary body also is visible (Fig. 6B). Low magnification images in Figure 7 indicate the locations of

ciliary muscle and iris sphincter muscle imaging of immunolabeled structures in Figure 8. Immunohistochemistry demonstrated that all five mAChR subtypes tested (1–5) are present in the iris and ciliary muscle, as well as in the retina, which is included for comparative purposes. As shown in Figure 8, staining for each receptor subtype is present in all three tissues. Ciliary muscle images were captured from the longitudinal muscle, and iris images from the pupillary margin. Results for control conditions rule out the possibility of nonspecific staining and autofluorescence as alternative explanations. Specifically, control sections washed in a solution of primary antibody/synthetic receptor showed significantly less fluorescence for all receptor subtypes and all tissues examined, and unstained ciliary body sections showed minimal autofluorescence. Qualitative estimates of the relative intensity of labeling in experimental sections compared to the control sections are provided in Table 2. In the ciliary muscle, receptor types M3 and M5 have the strongest staining, while staining for type M3 receptors appears strongest in the iris. Raw images are shown in the Supplementary Figures.

DISCUSSION

Reports that cycloplegia in guinea pigs results in hyperopic shifts in refractive errors[1] imply that they can accommodate. The results from in vivo pharmacological experiments reported here confirmed accommodative activity in the guinea pig. The baseline data collected in this study also provided a perspective on developmental changes in the anterior segment in the guinea pig eye.

In humans and nonhuman primates, accommodation is attributable largely to changes in the shape of the crystalline lens, initiated by contraction of the ciliary muscle, which releases tension on zonular fibers, thereby allowing the lens to thicken, its surfaces to steepen, and its dioptric power to increase. In addition to these lens shape changes, the anterior chamber becomes shallower. A similar decrease in ACD was observed in our guinea pigs following pilocarpine instillation, as evident in A-scan ultrasonography and anterior segment OCT imaging data. However, minimal lens thickening was observed by A-scan ultrasonography in vivo, following pilocarpine instillation, and in vitro testing yielded no evidence of lens curvature changes in response to carbachol. We also found no evidence of drug-induced corneal curvature changes in the guinea pig, although significant corneal steepening during accommodation has been reported in chicks and some other avian species,[12,29] and there have been isolated reports of corneal accommodation in humans.[30,31]

Taken together, the above observations suggested translational and deformational contributions to accommodation in the guinea pig. In support of the former, a significant decrease in ACD was found. Lens shape changes during accommodation cannot be ruled out, given that some animals also showed increases in LT in response to applied pilocarpine. This observation, along with the finding that the position of the posterior lens surface did not change during accommodation, even though the ACD decreased, implies lens thickening and, thus, a shape change.

Some caution is warranted in interpreting the data reported here. First, it should be noted that repeated dosing with pilocarpine in vivo and a high concentration of carbachol in vitro were required to elicit the above accommodative changes, suggesting that the ciliary muscle in the guinea pig is relatively underdeveloped in comparison with that of monkeys and humans.[14,32] Second, there was significant variability in our in vivo data with respect to the changes in ACD and LT. In relation to the latter, two animals demonstrated
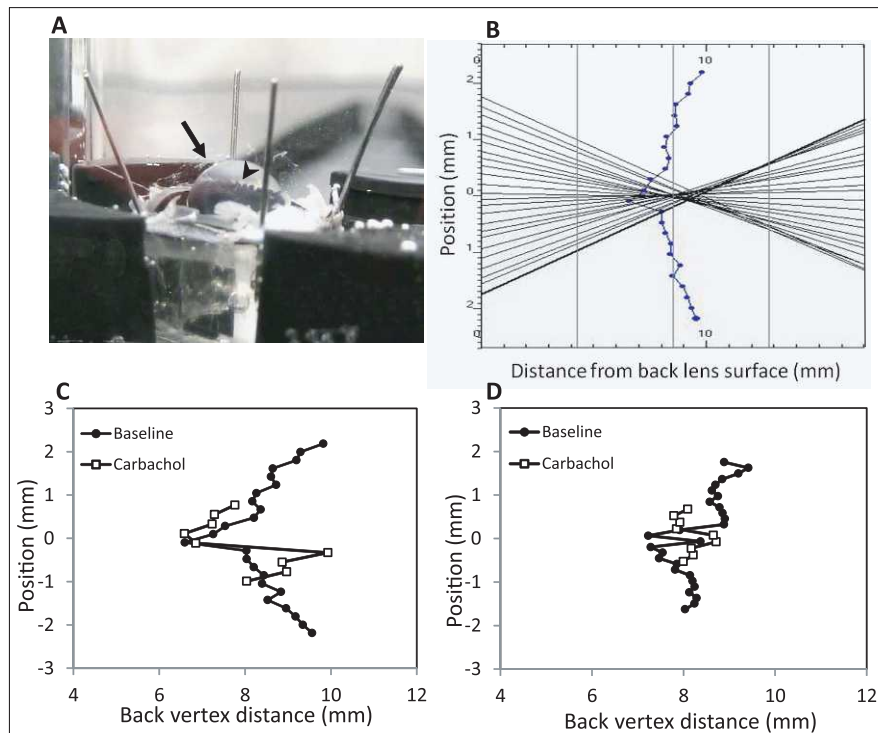
FIGURE 5. (A) Anterior segment preparation used for in vitro lens scanning; laser scans vertically from below, through the cornea (not shown) and lens; *arrow* shows posterior lens surface; ciliary processes also visible through the lens (*arrowhead*). (B) Scan showing the path of individual rays passing through a guinea pig cornea-lens complex before addition of carbachol to bath, with calculated BVD at each position superimposed (*line with dots*); 0 position on *y*-axis represents the optical center of the lens; (C, D) represent two examples obtained before, and 20 minutes after, the addition of 10 mM carbachol solution (● – baseline, □ – after carbachol).

a decrease in LT, while four animals demonstrated an increase. The very small size of the induced changes combined with the steep profile of the posterior lens surface of the guinea pig eye likely contributed to the variability; thus, even with the high resolution of the techniques used for measurements, any small amount of misalignment would have contributed significant noise. Increasing the number of animals tested may have helped to decrease the variability in the data, but is not expected to have altered the experimental outcome. It also is possible that lens shape, that is, deformational, changes are an age-dependent feature of guinea pig accommodation; further studies with an increased number of animals spanning the ages already studied are warranted to address this possibility.

There is some debate as to whether the lens as a whole undergoes an anterior translational movement during accommodation in humans and monkeys. A study in children found anterior translational movements of anterior and posterior lens surfaces during accommodation of hyperopes.[33] However, other studies in humans suggest that the posterior lens surface moves posteriorly, not anteriorly, during accommodation.[34,35] Evaluating the posterior lens surface using optical methods can be influenced by a change in refractive index of the lens with accommodation.[36] While some of our data fit with a lens translational model for accommodation in the guinea pig, as noted above, we also cannot rule out a deformational change in the lens, presumably involving an increase in anterior lens surface curvature. Nonetheless, the results of our in vitro experiments imply that any such deformational changes are very small, if present.

In comparing results from our in vivo and in vitro experiments, it is important to recognize that the lens scanning technique applied in the latter makes use of isolated anterior segment preparations and it is possible to detect only lens

curvature-related changes. The removal of the posterior vitreous chamber and associated structures eliminates any potential contribution to accommodation from such structures. Furthermore, as the globe is no longer intact, by default any potential for the anterior vitreous to exert pressure on the lens-ciliary body complex and so to contribute to lens translation is eliminated.[37] This lens scanning technique has been used successfully to document robust LT and curvature changes with nicotine in preparations from chicken eyes.[12] Related studies also revealed a role for the iris in accommodation in the chicken; when the iris was removed before testing, the lens lost its ability to undergo deformational changes. Given that we saw no evidence of lens shape changes, we had no reason to undertake further testing of iridectomized preparations. However, as in our previous studies involving chicks, we observed robust pupil constriction in the guinea pig preparations. This response provided a readily accessible index of tissue viability. It also has important optical implications as discussed further below.

Our in vitro studies revealed significant negative spherical aberration in the guinea pig lens, with the pupil having an important modulating influence. Specifically, by eliminating more peripheral rays, pupil constriction led to an apparent reduction in negative spherical aberration, with the net effect of moving the mean posterior focal plane toward the lens. The implications of such a change for the intact eye would be an apparent myopic shift in refractive error or "pseudo-accommodation." This pupillary effect could have functional benefits for the guinea pig, whose true accommodative ability appears to be modest, at best, although a study of awake behaving guinea pigs is required to test this notion. As an aside, pupil size changes can be ruled out as the explanation for pilocarpine-induced changes in refraction observed in vivo,
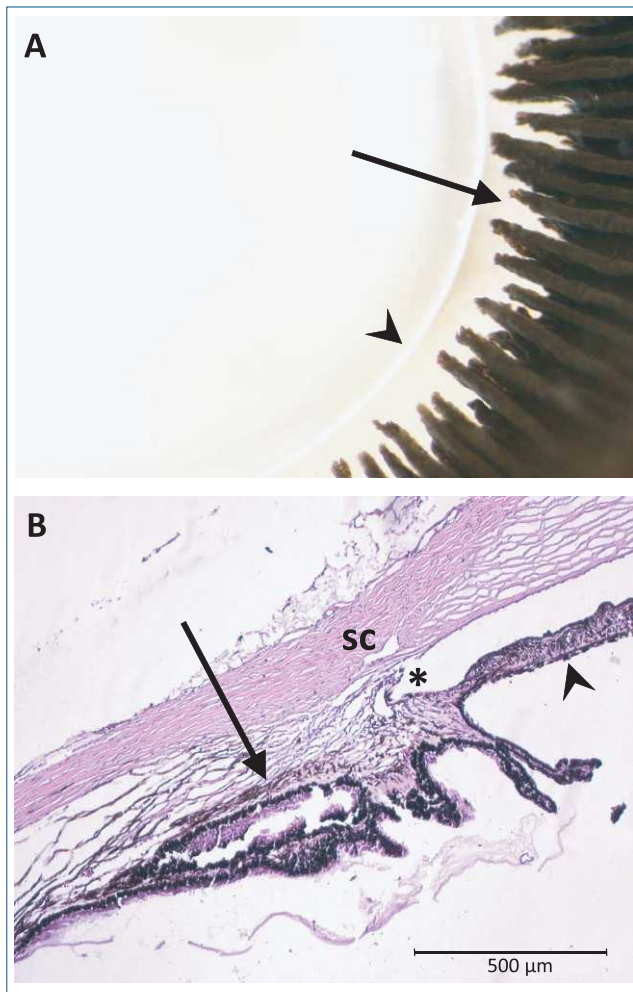
FIGURE 6. (A) Gross morphology of the lens and ciliary processes viewed from the posterior side; *arrowhead* indicates lens equator and *arrow* indicates ciliary processes (B) H&E-stained section of the iridocorneal angle. *Arrow* indicates longitudinal ciliary muscle and *arrowhead* indicates posterior iris. *Angle. SC, Schlemm's canal.

with more steeply curved posterior surfaces relative to human and nonhuman primate lenses.[38] Thus, rodent lenses can be expected to require more force to stretch and compress. On the other hand, these high-powered lenses only need to undergo small changes in position to effect significant ocular dioptric power changes. This is exemplified by our in vivo data showing approximately 5 D changes in refraction, for 0.02- to 0.05-mm change in ACD. As a potential explanation for the apparent lack of accommodation in mice, it is possible that the combination of a very thick lens and a very small eye precludes lens movement; the large depth of focus afforded by its small eye and very poor visual resolution also reduce the need for accommodation.

In evolutionary terms, the guinea pig, being a member of the rodent family, would not be expected to possess a large accommodative amplitude. However, unlike many other animals in the rodent family, they are considered diurnal animals, although they show no clear circadian heart rate rhythmicity,[39] and they can be active both during the day and night. The relatively modest accommodation ability (~5 D amplitude) of the guinea pig is consistent with their visual needs, taking into consideration their foraging habits, and the additional finding that the lower visual field in guinea pigs is relatively myopic compared to the superior visual field by approximately 5 D.[40] This refractive error gradient would serve to complement any active accommodation in bringing into focus nearby objects on the ground, as will any near-associated pupillary constriction, for reasons outlined above.

Over the age range of the guinea pigs used in this study (2 to 16 months), we did not detect any age-related decline in accommodation, although biometric data confirmed age-related increases in baseline ACD and LT. However, as noted above, our sample size is small. Nonetheless, this result also is not surprising, given that presbyopia, as documented in humans[14] and nonhuman primates,[41] is, at least in part, due to increases in stiffness of the crystalline lens.[42–44] While significant age-related stiffening also has been described for many mammals, including the mouse[21] and pig,[45] such changes are expected to have less impact on the accommodation ability of an animal in which lens translation dominates over shape changes, which we suggest is the case for the guinea pig.

In vitro lens scanning experiments revealed a strong meiotic response to carbachol, which also was observed in vivo with pilocarpine. These results, together with the pilocarpine-induced decrease in ACD, provide indirect evidence for the presence of muscarinic receptors on the iris sphincter and ciliary muscles of guinea pigs. In humans, all five muscarinic AChR subtypes (M1–5) have been found in the ciliary body and iris, with the M3 receptor being the
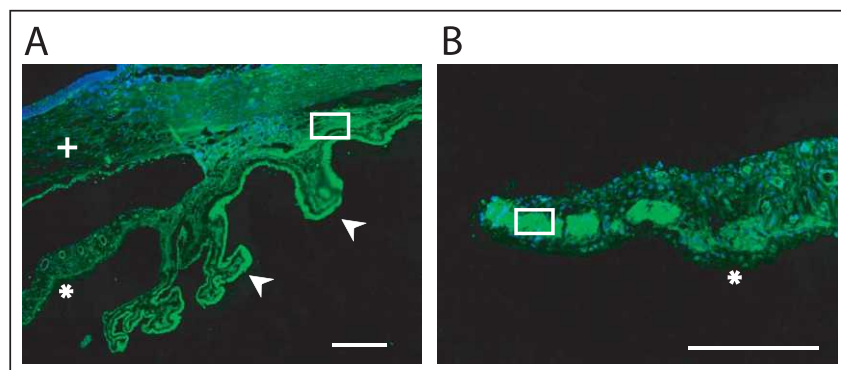
because of the fixed pupil area sampled in the autorefraction technique used to collect these data.

Our conclusion that guinea pigs can accommodate contrasts with the suggestions that the mouse, another rodent, has no accommodation.[21] In both cases, and as typical of rodent eyes, they have very thick lenses relative to their ocular length,

FIGURE 7. Low magnification images (DAPI, *blue*; FITC, *green*) showing the location of (A) longitudinal ciliary muscle and (B) iris sphincter muscle used for imaging immunolabeling. *Arrowheads* indicate ciliary processes. +Cornea. *Posterior iris. *Scale bars*: 200 μM.
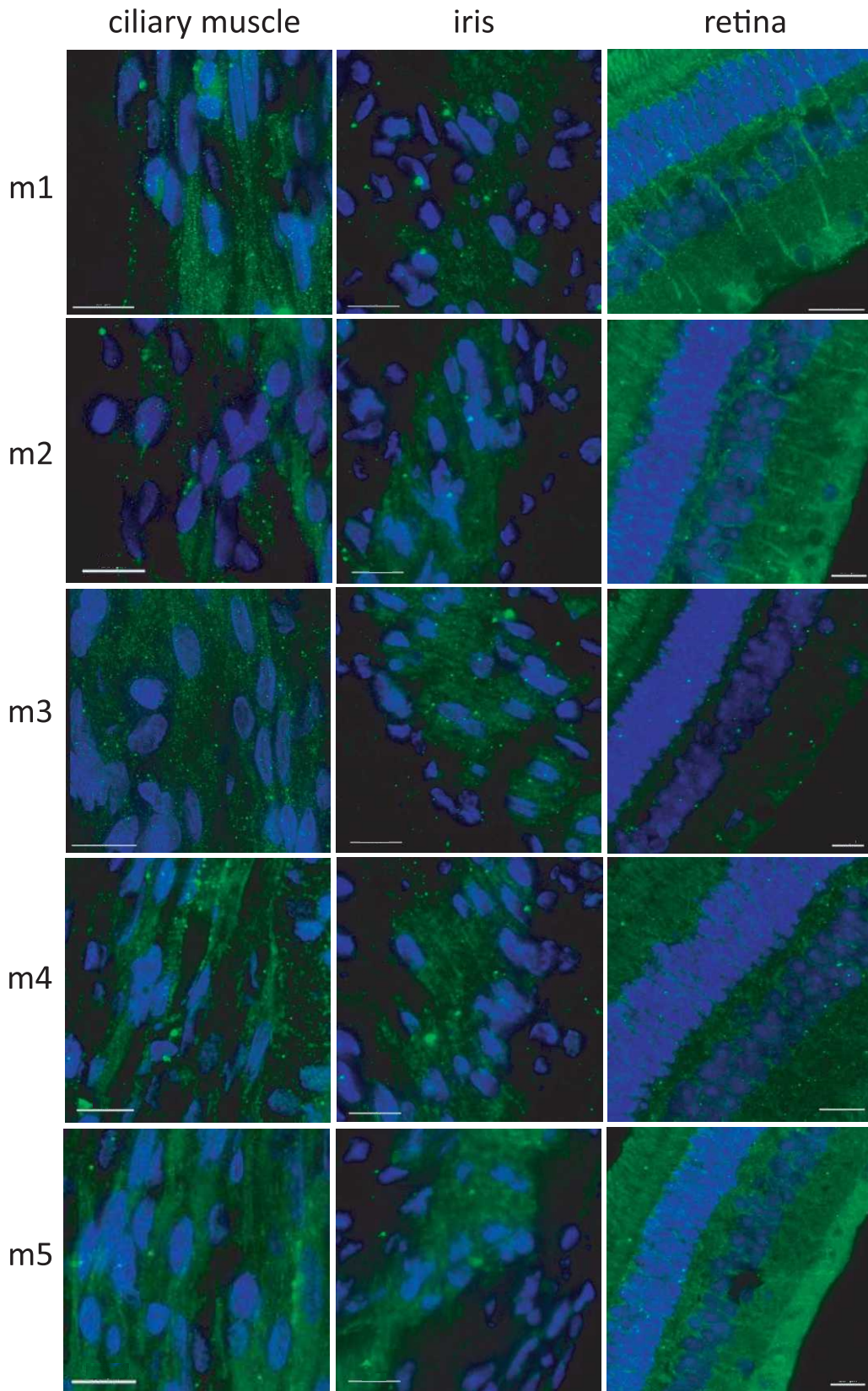
Figure 8. Guinea pig ocular tissues immunolabeled for muscarinic receptors M1 to M5. DAPI (*blue*) and IgG-conjugated (FITC, *green*). *Scale bars*: 15 μM.

TABLE 2. Intensity of Immunolabeling for M1 to M5 in Ciliary Muscle, Iris and Retina as Compared to Control Sections With Matched Intensity (See Supplementary Figs.)

Muscarinic Receptor Subtype	Ocular Tissue		
	Ciliary Muscle	Iris	Retina
M1	++	++	+ PRL, OPL, IPL
M2	++	+	++ PRL, OPL, NFL
M3	+++	+++	++ IPL, OPL, NFL
M4	++	++	+ IPL, OPL, NFL
M5	+++	+	+ OPL, IPL +++ NFL

Distribution of staining in the retina is shown. PRL, photoreceptor layer; NFL, nerve fiber layer; +++, highest specific staining; +, lowest specific staining.

predominant subtype.[46–48] All five mAChR subtypes also have been found in the tree shrew iris and ciliary body.[49] In an already published study in guinea pig, all five mAChR subtypes were reported to be present in the iris–ciliary body complex, based on results from RT-PCR and Western blotting, for which M3 receptors produced the most intense immunoreactive band.[22] Our immunohistochemistry results for M1 to M5 receptors are consistent with the latter report, and also in more general terms, with pupil and accommodation data reported here.

As an independent test of the specificity of our antibodies, retinal tissue also was processed for immunohistochemistry. All five subtypes of muscarinic receptors (M1-5) were found in retinal sections, although they varied in their distribution patterns, as documented in Table 2. Similar results have been reported for rabbits and tree shrews. In rabbits, all five muscarinic receptor subtypes were shown to be present in the retina, with a predominance of M3 staining in the outer plexiform (OPL) and inner nuclear (INL) layers, as well as M2 and M5 in bipolar cells, and a broad distribution of all subtypes through the inner retina.[50] In tree shrew, M1 were found to be present in the OPL and IPL, M2 in the photoreceptor outer segments, OPL, IPL, and NFL, and M3 in the OPL and NFL, with processes extending to IPL.[49] These data also are of relevance to studies investigating the antimyopia actions of antimuscarinic drugs, in that they offer insight into potential sites of action and confounding ocular side-effects.

As a final aside, it should be noted that the pupillary light reflex and, thus, pupil size may be affected by the ketamine/xylazine anesthesia protocol used in the current study.[51] However, it is unlikely that it affected the pupillary responses recorded in vivo. First, at doses up to 40 mg/kg ketamine and 17 mg/kg xylazine, studies in mice showed that pupil size and the pupillary light reflex were unaffected.[52–54] Second, the reported pupil size changes reflect direct interactions between the applied drug and receptors on the sphincter muscle, and, thus, are not dependent on the functional state of the pupillary light reflex pathway.

In conclusion, we found changes in refraction, ACD and pupil size in response to muscarinic agonist drugs, consistent with the presence of muscarinic receptors on the iris and ciliary body musculature of the guinea pig eye and ocular accommodation, which appears to be a product of a translational movement and a deformational change of the crystalline lens. While the guinea pig's accommodation ability is only modest, nonetheless, the potential for its accommodation to modulate the retinal defocus experience of young guinea pigs wearing myopia-inducing negative lenses cannot be ignored.

References

1. Howlett MH, McFadden SA. Form-deprivation myopia in the guinea pig (Cavia porcellus). *Vision Res*. 2006;46:267–83.
2. Howlett, MH McFadden SA. Spectacle lens compensation in the pigmented guinea pig. *Vision Res*. 2009;49:219–27.
3. McFadden SA, Howlett MH, Mertz JR. Retinoic acid signals the direction of ocular elongation in the guinea pig eye. *Vision Res*. 2004;44:643–53.
4. Howlett MH, McFadden SA. Emmetropization and schematic eye models in developing pigmented guinea pigs. *Vision Res*. 2007;47:1178–1190.
5. Jiang L, Schaeffel F, Zhou X, et al. Spontaneous axial myopia and emmetropization in a strain of wild-type guinea pig (Cavia porcellus). *Invest Ophthalmol Vis Sci*. 2009;50:1013–1019.
6. Choh V, Sivak JG, Meriney SD. A physiological model to measure effects of age on lenticular accommodation and spherical aberration in chickens. *Invest Ophthalmol Vis Sci*. 2002;43:92–98.
7. Glasser A, Kaufman PL. The mechanism of accommodation in primates. *Ophthalmology*. 1999;106:863–872.
8. Cottriall CL, McBrien NA. The M1 muscarinic antagonist pirenzepine reduces myopia and eye enlargement in the tree shrew. *Invest Ophthalmol Vis Sci*. 1996;37:1368–79.
9. Troilo D, Wallman J. Changes in corneal curvature during accommodation in chicks. *Vision Res*. 1987;27:241–247.
10. Glasser A, Murphy CJ, Troilo D, Howland HC. The mechanism of lenticular accommodation in chicks. *Vision Res*. 1995;35:1525–1540.
11. Schaeffel F, Howland HC. Corneal accommodation in chick and pigeon. *J Comp Physiol A*. 1987;160:375–384.
12. Ostrin LA, Liu Y, Choh V, Wildsoet CF. The role of the iris in chick accommodation. *Invest Ophthalmol Vis Sci*. 2011;52:4710–4716.
13. McBrien NA, Moghaddam HO, New R, Williams LR. Experimental myopia in a diurnal mammal (Sciurus carolinensis) with no accommodative ability. *J Physiol*. 1993;469:427–441.
14. Ostrin LA, Glasser A. Accommodation measurements in a prepresbyopic and presbyopic population. *J Cataract Refract Surg*. 2004;30:1435–1444.
15. Faulkner AE, Kim MK, Iuvone PM, Pardue MT. Head-mounted goggles for murine form deprivation myopia. *J Neurosci Methods*. 2007;161:96–100.
16. Barathi VA, Boopathi VG, Yap EP, Beuerman RW. Two models of experimental myopia in the mouse. *Vision Res*. 2008;48:904–916.
17. Pardue MT, Faulkner AE, Fernandes A, et al. High susceptibility to experimental myopia in a mouse model with a retinal on pathway defect. *Invest Ophthalmol Vis Sci*. 2008;49:706–712.

18. Tekin M, Chioza BA, Matsumoto Y, et al. SLITRK6 mutations cause myopia and deafness in humans and mice. *J Clin Invest*. 2013;123:2094–2102.

19. Song YZ, Zhao YY, Zhang FJ. [The progression of applying transgenic mice as an animal model of high myopia]. *Zhonghua Yan Ke Za Zhi*. 2013;49:377–380.

20. Hsi E, Chen KC, Chang WS, et al. A functional polymorphism at the FGF10 gene is associated with extreme myopia. *Invest Ophthalmol Vis Sci*. 2013;54:3265–3271.

21. Baradia H, Nikahd N, Glasser A. Mouse lens stiffness measurements. *Exp Eye Res*. 2010;91:300–7.

22. Liu Q, Wu J, Wang X, Zeng J. Changes in muscarinic acetylcholine receptor expression in form deprivation myopia in guinea pigs. *Mol Vis*. 2007;13:1234–1244.

23. Bognar IT, Wesner MT, Fuder H. Muscarine receptor types mediating autoinhibition of acetylcholine release and sphincter contraction in the guinea-pig iris. *Naunyn Schmiedebergs Arch Pharmacol*. 1990;341:22–29.

24. Cardelus I, Anton F, Beleta J, Palacios JM. Anticholinergic effects of desloratadine, the major metabolite of loratadine, in rabbit and guinea-pig iris smooth muscle. *Eur J Pharmacol*. 1999;374:249–254.

25. Nickla DL, Wildsoet C, Wallman J. Visual influences on diurnal rhythms in ocular length and choroidal thickness in chick eyes. *Exp Eye Res*. 1998;66:163–181.

26. Richdale K, Bailey MD, Sinnott LT, et al. The effect of phenylephrine on the ciliary muscle and accommodation. *Optom Vis Sci*. 2012;89:1507–1511.

27. Kuchem MK, Sinnott LT, Kao CY, Bailey MD. Ciliary muscle thickness in anisometropia. *Optom Vis Sci*. 2013;90:1312–1320.

28. Williams HP. Comparison of the accommodative effects of carbachol and pilocarpine with reference to accommodative esotropia. *Br J Ophthalmol*. 1974;58:668–673.

29. Pardue MT, Sivak JG. The functional anatomy of the ciliary muscle in four avian species. *Brain Behav Evol*. 1997;49:295–311.

30. Yasuda A, Yamaguchi T, Ohkoshi K. Corneal steepening during accommodation. *J Cataract Refract Surg*. 2004;30:1611–1612.

31. Yasuda A, Yamaguchi T, Ohkoshi K. Changes in corneal curvature in accommodation. *J Cataract Refract Surg*. 2003;29:1297–1301.

32. Ostrin LA, Glasser A. Edinger-Westphal and pharmacologically stimulated accommodative refractive changes and lens and ciliary process movements in rhesus monkeys. *Exp Eye Res*. 2007;84:302–313.

33. Kaluzny BJ. Anterior movement of the crystalline lens in the process of accommodation in children. *Eur J Ophthalmol*. 2007;17:515–520.

34. Baikoff G, Lutun E, Wei J, Ferraz C. Anterior chamber optical coherence tomography study of human natural accommodation in a 19-year-old albino. *J Cataract Refract Surg*. 2004;30:696–701.

35. Beauchamp R, Mitchell B. Ultrasound measures of vitreous chamber depth during ocular accommodation. *Am J Optom Physiol Opt*. 1985;62:523–532.

36. Dubbelman M, van der Heijde GL, Weeber HA. The thickness of the aging human lens obtained from corrected Scheimpflug images. *Optom Vis Sci*. 2001;78:411–416.

37. Coleman DJ. Unified model for accommodative mechanism. *Am J Ophthalmol*. 1970;69:1063–1079.

38. Zamudio AC, Candia OA. Interaction between mechanical and osmotic forces in the isolated rabbit lens. *Exp Eye Res*. 2011; 93:798–803.

39. Akita M, Ishii K, Kuwahara M, Tsubone H. The daily pattern of heart rate, body temperature, and locomotor activity in guinea pigs. *Exp Anim*. 2001;50:409–415.

40. Zeng G, Bowrey HE, Fang J, Qi, Y, McFadden SA. The development of eye shape and the origin of lower field myopia in the guinea pig eye. *Vision Res*. 2013;76:77–88.

41. Wendt M, Croft MA, McDonald J, Kaufman PL, Glasser A. Lens diameter and thickness as a function of age and pharmacologically stimulated accommodation in rhesus monkeys. *Exp Eye Res*. 2008;86:746–572.

42. Glasser A, Campbell MC. Presbyopia and the optical changes in the human crystalline lens with age. *Vision Res*. 1998;38: 209–229.

43. Heys KR, Cram SL, Truscott RJ. Massive increase in the stiffness of the human lens nucleus with age: the basis for presbyopia? *Mol Vis*. 2004;10:956–963.

44. Weeber HA, Eckert G, Soergel F, et al. Dynamic mechanical properties of human lenses. *Exp Eye Res*. 2005;80:425–434.

45. Kammel R, Ackermann R, Mai T, Damm C, Nolte S. Pig lenses in a lens stretcher: implications for presbyopia treatment. *Optom Vis Sci*. 2012;89:908–915.

46. Gupta N, Drance SM, McAllister R, et al. Localization of M3 muscarinic receptor subtype and mRNA in the human eye. *Ophthalmic Res*. 1994;26:207–213.

47. Gil DW, Krauss HA, Bogardus AM, WoldeMussie E. Muscarinic receptor subtypes in human iris-ciliary body measured by immunoprecipitation. *Invest Ophthalmol Vis Sci*. 1997;38: 1434–1442.

48. Zhang X, Hernandez MR, Yang H, Erickson K. Expression of muscarinic receptor subtype mRNA in the human ciliary muscle. *Invest Ophthalmol Vis Sci*. 1995;36:1645–1657.

49. McBrien NA, Jobling AI, Truong HT, Cottriall CL, Gentle A. Expression of muscarinic receptor subtypes in tree shrew ocular tissues and their regulation during the development of myopia. *Mol Vis*. 2009;15:464–475.

50. Strang CE, Renna JM, Amthor FR, Keyser KT. Muscarinic acetylcholine receptor localization and activation effects on ganglion response properties. *Invest Ophthalmol Vis Sci*. 2010;51:2778–2789.

51. Eilers H, Larson MD. The effect of ketamine and nitrous oxide on the human pupillary light reflex during general anesthesia. *Auton Neurosci*. 2010;152:108–114.

52. Aleman TS, Jacobson SG, Chico JD, et al. Impairment of the transient pupillary light reflex in Rpe65(-/-) mice and humans with leber congenital amaurosis. *Invest Ophthalmol Vis Sci*. 2004;45:1259–1271.

53. Pennesi ME, Lyubarsky AL, Pugh EN Jr. Extreme responsiveness of the pupil of the dark-adapted mouse to steady retinal illumination. *Invest Ophthalmol Vis Sci*. 1998;39:2148–2156.

54. Grozdanic S, Sakaguchi DS, Kwon YH, Kardon RH, Sonea IM. Characterization of the pupil light reflex, electroretinogram and tonometric parameters in healthy rat eyes. *Curr Eye Res*. 2002;25:69–78.